

Nanoscale thermal–mechanical probe determination of ‘softening transitions’ in thin polymer films*

Jing Zhou, Brian Berry, Jack F Douglas, Alamgir Karim, Chad R Snyder and Christopher Soles

Polymers Division, National Institute of Standards and Technology, 100 Bureau Drive, Gaithersburg, MD 20899-8541, USA

E-mail: alamgir.karim@nist.gov and csoles@nist.gov

Received 27 August 2008, in final form 8 October 2008

Published 19 November 2008

Online at stacks.iop.org/Nano/19/495703

Abstract

We report a quantitative study of the softening behavior of glassy polystyrene (PS) films at length scales on the order of 100 nm using nano-thermomechanometry (nano-TM), an emerging scanning probe technique in which a highly doped silicon atomic force microscopy (AFM) tip is resistively heated on the surface of a polymer film. The apparent ‘softening temperature’ T_s of the film is found to depend on the logarithm of the square root of the thermal ramping rate R . This relation allows us to estimate a quasi-equilibrium (or zero rate) softening transition temperature T_{s0} by extrapolation. We observe marked shifts of T_{s0} with decreasing film thickness, but the nature of these shifts, and even their sign, depend strongly on both the thermal and mechanical properties of the supporting substrate. Finite element simulations suggest that thin PS films on rigid substrates with large thermal conductivities lead to increasing T_{s0} with decreasing film thickness, whereas softer, less thermally conductive substrates promote reductions in T_{s0} . Experimental observations on a range of substrates confirm this behavior and indicate a complicated interplay between the thermal and mechanical properties of the thin PS film and the substrate. This study directly points to relevant factors for quantitative measurements of thermophysical properties of materials at the nanoscale using this nano-TM based method.

 Supplementary data are available from stacks.iop.org/Nano/19/495703

(Some figures in this article are in colour only in the electronic version)

1. Introduction

Materials patterned into nanostructures or multiphase materials with nanoscale domains (e.g., block copolymers, polymer blends [6, 28, 17, 3, 21, 27], or nanocomposites [8, 1, 2, 15]) are the cornerstone for many emerging applications in nanotechnology. In many instances, one would like to probe the thermal properties of these systems that are heterogeneous at the nanoscale. This requires a local thermal analysis technique with nanometer resolution. Conventional calorimetry techniques such as differential

scanning calorimetry (DSC) require several milligrams of sample to obtain a reasonable signal-to-noise ratio. Localized thermal probe measurements using a Wollaston wire based scanning tip have been reported [18, 19, 7]. Typically, a 5 μm diameter wire is bent into a tip with 20 μm radius of curvature. This system is not suitable for thermal analysis at sub- μm length scales. Nano-thermomechanometry (nano-TM) has recently emerged as a possible technique for quantitative nano-thermal analysis [12, 11]. King *et al* have pioneered this technique, which utilizes a highly doped Si AFM tip that is resistively heated [16]. With proper calibration, this nano-TM technique has the potential to determine the melting point (T_m) or the glass transition temperature (T_g) of a material at the nanoscale. Nano-TM measures the cantilever deflection

* The error bars presented throughout the manuscript indicate the relative standard uncertainty of the measurement.

of the AFM tip as the tip temperature is increased. A sharp deflection of the tip into the material occurs at a specific ‘softening temperature’ that is presumably related to either the T_g or T_m of the material being tested. To date, nano-TM is the only technique that allows spatially resolved measurement of thermophysical properties at nanometer length scales. However, the ‘softening’ transition in thin polymer films is distinct from bulk glass formation since the properties of these films are related non-trivially to the supporting solid substrate below the film and to the environment above it by thermal and mechanical couplings. Thus, the interpretation of the softening temperature in nano-TM is complicated by a number of factors.

In the present paper, we focus on the nano-TM measurements of the softening temperature T_s of amorphous thin polymer films, which has evident technological significance in materials science and nanotechnology. Specifically, we are concerned with basic factors that influence T_s , such as the film thickness and the thermal and mechanical properties of the substrate on which the film is supported. Previous observations with this thermal probe method have led to many contradictory observations, so there is a need to establish a firmer foundation for the interpretation of these measurements. Our analysis indicates that there are two principal factors that have influenced previous disparate estimates of nano-TM softening temperatures. One factor is the thermal transport through the interface of thin films (order of 100–500 nm) to the film substrate. The other basic factor is the redistribution of the stress fields within the films and substrate due to the existence of interfaces. We find below that both these thermal and mechanical coupling effects are intricately convoluted in the nano-TM measurement.

2. Materials and methods

The equipment and instruments or materials are identified in this paper in order to adequately specify the experimental details. Such identification does not imply recommendation by NIST, nor does it imply that the materials are necessarily the best available for the purpose.

2.1. Materials and sample preparation

The PS (Scientific Polymer Products Inc.) used in our study has two molar masses¹: $M_{r,w} = 19.3 \text{ kg mol}^{-1}$ ($M_{r,w}/M_{r,n} = 1.07$) and $M_{r,w} = 1571 \text{ kg mol}^{-1}$ ($M_{r,w}/M_{r,n} = 1.03$), where $M_{r,w}$ is the relative mass averaged molar mass and $M_{r,n}$ is the relative number averaged molar mass. The PS films were obtained by spin-casting from its toluene solution on pre-cleaned Si and glass substrates. The Si substrate was treated by an ultraviolet/ozone cleaner (Model 342, Jelight) for 1 min. The glass substrate was cleaned by ultrasonication in acetone

and isopropanol for 10 min each, and then plasma treated for 5 min to remove the organic residuals. After spin-casting, these films were annealed in a vacuum oven at 150 °C for ≈ 2.5 h to release the residual stress at the film/substrate interface. The film thickness was measured by a UV-visible interferometer (Model F20, Filmetrics) operated in reflectance mode. The PS films were transferred from Si wafers onto PDMS substrates. The PDMS was prepared by the suggested procedure from the manufacturer (Sylgard 184, Dow Corning): mixing the base and the curing agent at the ratio of 10:1 by mass. The mixed solution was cured in an oven at 70 °C for ≈ 2 h after being degassed under vacuum for ≈ 1 h. The Si wafer was treated under UV/ozone for 10 min to make the surface hydrophilic before spin-casting. A cured PDMS sheet was placed onto a freshly made Si supported PS film, which was then immersed in water. Water wets the interface between the hydrophilic wafer and polymer film, thereby transferring the polymer films to the PDMS. These procedures resulted in high quality films with surfaces that appeared to be optically mirror smooth. Both x-ray reflectivity and atomic force microscopy revealed that the roughness of the PS, PDMS, and Si surfaces was on the order of a few nanometers or less.

2.2. Nano-thermomechanometry method

Nano-thermomechanometry (nano-TM) experiments were conducted using an AFM (Asylum Research MFP-3D) system equipped with a power controller (Anasys Instruments Nano-TA) used to heat the nano-TM tip (Anasys Instruments). The input voltage and tip temperature relation of every tip was calibrated individually by measuring the transition temperature of several standard polymers with known melting temperatures, i.e., polycaprolactone ($T_m = 55$ °C), polyethylene ($T_m = 116$ °C), and polyethylene terephthalate ($T_m = 235$ °C). Such a calibration process is assumed to eliminate or reduce the thermal contact problem, but it cannot be perfect. During nano-TM measurements, the tip temperature started from 75 °C and was ramped up at different rates. When it reached a temperature about (5–10) °C higher than the transition temperature, the voltage was held constant and the tip started to retract from the sample surface. Once the tip was fully withdrawn from the sample surface, the voltage was ramped down to allow the tip to cool down to room temperature. All the sampling zone was spatially located far enough apart to avoid the interference of surface deformation from previous tests.

The stiffness of the AFM cantilever beam changes with temperature due to the thermal expansion of the lever and the variation of the elastic modulus with temperature. In order to minimize the influence of the stiffness change in our measurements, we performed a calibration on every cantilever/AFM tip at the beginning of each experiment. First, the cantilever was freely suspended in air, while the tip temperature was ramped up in the same manner as for nano-TM experiments. Second, the deflection voltage of the cantilever beam was recorded as a function of the tip temperature. In general, the change of deflection voltage is less than 10% of the total deflection voltage change in the actual

¹ According to ISO 31-8, the term ‘molecular weight’ has been replaced by ‘relative molecular mass’, symbol M_r . Thus, if this nomenclature and notation were to be followed in this publication, one would write $M_{r,w}$ instead of the historically conventional M_w for the mass average molecular weight, with similar changes for M_n , M_z and M_v , and it would be called the ‘mass average relative molecular mass’. The conventional notation, rather than the ISO notation, has been employed for this publication.

nano-TM measurements. Finally, the recorded deflection voltage curve was subtracted from the measurement curve before we determined the transition temperatures. Based upon these observations, there was no alteration of the transition temperature compared to uncorrected data.

2.3. Finite element simulation

All finite element method (FEM) simulations were conducted with ABAQUS 6.6-3. The model used for the thermal dissipation simulation was PS films ($t = (100, 200 \text{ and } 500) \text{ nm}$) on $500 \mu\text{m}$ Si, glass and PDMS substrates (figure S5 in supporting materials (available at stacks.iop.org/Nano/19/495703)). The material properties used in the FEM simulations are summarized in table S1 (available at stacks.iop.org/Nano/19/495703). All boundaries were considered to exchange heat with the surroundings through surface convection. In this case, the heat flux on the surface is governed by $q = -h(\theta - \theta^\circ)$, where q is the heat flux across the surface, h the film coefficient, θ the temperature on the surface at this point, and θ° the sink temperature. The heat input is only from the tip-sample contact interface, which is defined as a heat source with 50 nm radius, which is determined from the AFM measurement of the surface at different temperatures (figure S6 in supporting materials (available at stacks.iop.org/Nano/19/495703)). The temperature of the heat source was ramped from 75 to 103°C at a varying rate of $2\text{--}20^\circ\text{C s}^{-1}$. The heat dissipation inside the system is considered as an uncoupled transient heat transfer. The total heat loss from the tip-polymer contact interface is obtained by integrating the heat flux at each node in the direction normal to the film surface along the length of tip-polymer interface.

3. Results and discussion

Nano-TM is a variant of scanning probe microscopy, equipped with a custom designed heating tip. As shown in figure 1(a), the cantilever consists of two beams (dark) and the heating zone (bright) with a sharp monolithic tip. The beams are heavily doped by boron diffusion during the fabrication process, whereas the tip region is masked from this doping process. The result is that the electrical resistance of the beams is less than 10% of that of the tip, leading to higher heating in the tip region once the current passes through the entire cantilever. In the scanning electron micrograph (figure 1(b)), the low and high boron doped regions exhibit a sharply defined contrast. In this configuration, the tip temperature can be raised to $\approx 250^\circ\text{C}$ in a rate-controlled manner. In operation, a constant force ($\approx 5 \text{ nN}$) is applied to the cantilever against the sample (polymer film) while the mechanical deflection of the cantilever is monitored as the tip temperature is ramped up. This method probes a local area that reaches $\approx 100 \text{ nm}$ in the lateral dimensions, as indicated by the size of craters left on the polymer film after nano-TM tests. By contrast, the Wollaston scanning tip method has a typical resolution [18, 19, 7] on the order of $10 \mu\text{m}$ and thus cannot resolve the thermal response of a material at the nanoscale. In our experiments, multiple nano-TM scans were performed and all the data

discussed in this paper are statistically analyzed from four to six parallel tests. Figures 1(c) and (d) provide a 3D view and surface topography plot of the craters left behind after multiple nano-TM tests. Representative nano-TM traces are shown in figure 1(e), displaying four characteristic regions that are probed by the tip. First, the tip approaches and engages the sample surface under a pre-set force. Second, while ramping up the tip temperature, the cantilever deflects upward due to the thermal expansion of material underneath the tip. Finally, when the temperature reaches the characteristic softening temperature of the material T_s , the tip begins to indent into the specimen. In our experiment, T_s was extracted from the maximum of nano-TM curve where its first derivative equals zero.

One of the potential uses of the nano-TM technique is the routine identification of materials, even nanometer-sized specimens, based upon small differences in their thermophysical properties. The inset of figure 1(e) shows two films, A and B, with significantly different T_s . While both materials are polystyrene (PS), they differ in their molecular mass and corresponding T_g . The apparent T_g measured from the mid-point of the DSC trace is 100°C for A ($M_{r,w} = 19 \text{ kg mol}^{-1}$ PS) and 104°C for B ($M_{r,w} = 1571 \text{ kg mol}^{-1}$ PS). Nano-TM is evidently sensitive enough to perceive this small difference. This sensitivity, coupled with the ultra-small probing area (100 nm or less in diameter), indicates that nano-TM is a promising technique for the rapid thermal characterization of nanometer-sized materials and composites.

Despite its success in material identification, the temperature T_s often exhibits a significant deviation from the bulk glass transition temperature, T_g [16]. An obvious potential source of this discrepancy is the lag time for the heated tip to sink into the viscoelastic medium [20]. The localized heating of the sample by the nano-TM tip probe introduces a steep temperature gradient from the region near the tip to the surrounding environment. The alteration of viscosity caused by the temperature gradient creates a corresponding steep viscosity gradient that can vary by several orders of magnitude in the probed region. These sharp gradients result in a diminished polymer softening, which retards the deformation of the polymer film by the probing tip in the nano-TM experiments. The thermal and mechanical couplings of the probing tip to the film substrate are additional factors that can affect these measurements.

Thermal equilibrium can be difficult to achieve owing to very small heat capacity of a nanometer-sized specimen. As evidence of this, we observe a significant kinetic effect on the temperature ramping rate dependence of our T_s determination below, and T_s was also found to vary appreciably with film thickness, h_f . Our nano-TM experiments were performed on glassy PS thin films spun-cast on silicon substrates. As shown in figure 2(a), T_s increased with decreasing polymer h_f at any temperature ramping rate, R . Once h_f becomes smaller than 75 nm , however, T_s was not easily resolved (figure S1 in supporting materials (available at stacks.iop.org/Nano/19/495703)). We also found that changing R causes a steep change in T_s for low ramping rates, but this effect becomes weaker for the high ramping rate region

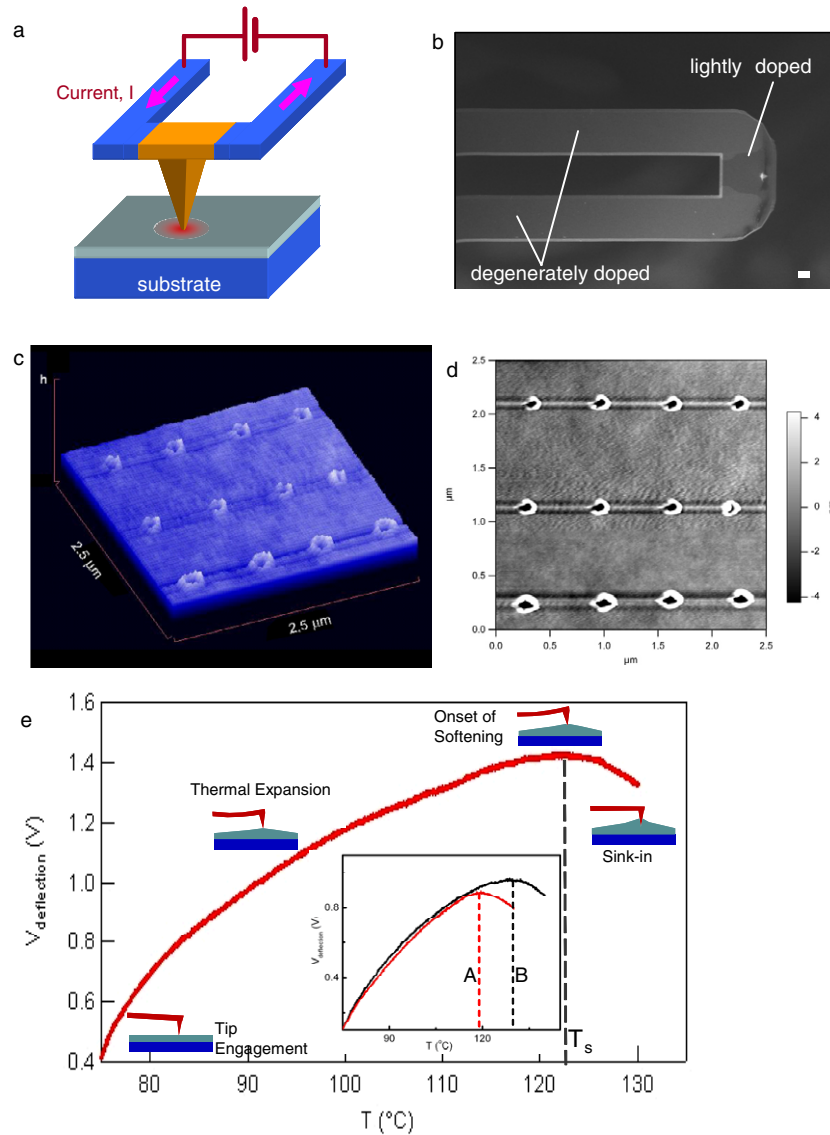


Figure 1. Mechanism of nano-thermomechanometry (nano-TM). (a) Schematic depiction of scanning probe microscope derived nano-TM for thin film analysis. (b) SEM images of a cantilever that consists of two heavily doped legs and a lightly doped heating zone in between. Scale bar: 5 μm . (c) 3D and (d) surface topography images of the craters generated by nano-TM testing. (e) Representative nano-TM curve for probing the thermal transition of polymer thin films. There are four stages in the time course of a full testing cycle, as depicted in the plot. The inset shows the capability of using nano-TM for fast material identification based upon thermophysical property differences.

(figure 2(b)). T_s at the ramping rate of $0.1\text{ }^\circ\text{C s}^{-1}$ is still far from quasi-steady state, but lowering the ramping rates below this value resulted in highly scattered observation. It is thus impractical to conduct nano-TM experiments at even lower ramping rates. After systematic analyses of all the rate dependent data under various conditions, we empirically observed that T_s logarithmically increased with the square root of R/R_0 , as

$$T_s = T_{s0} + B \log \left[\left(\frac{R}{R_0} \right)^{\frac{1}{2}} + 1 \right], \quad (1)$$

where R_0 is a empirical characteristic heating rate for the material and B is an adjustable fitting parameter (figure 2(c)). The motivation for using this empirical equation is to extract the quasi-equilibrium low temperature scanning rate limit

temperature, T_{s0} (figure 2(c) inset). R_0 was found to be approximately equal to $1\text{ }^\circ\text{C s}^{-1}$ for all the measurements. Over a relatively broad range ($0.1\text{--}20\text{ }^\circ\text{C s}^{-1}$), R_0 is only weakly linked to T_{s0} in the curve fitting. As noted above, we find that T_{s0} is strongly h_f dependent in the measured range ($100\text{--}500\text{ nm}$). Notice that these films are much thicker than those for which deviations in the apparent thin film T_g are normally observed [10], i.e., $h_f \leq 100\text{ nm}$. We next investigate why T_{s0} increases with decreasing film thickness and the physical properties of the film–substrate that influence shifts in T_{s0} .

First, we note that while equation (1) does an excellent job in numerically fitting our data, it is not intended to imply any physical mechanism for the T_s shift. This equation is only utilized to extrapolate the softening temperature T_s to its limiting value at an ‘infinitely slow’ heating rate.

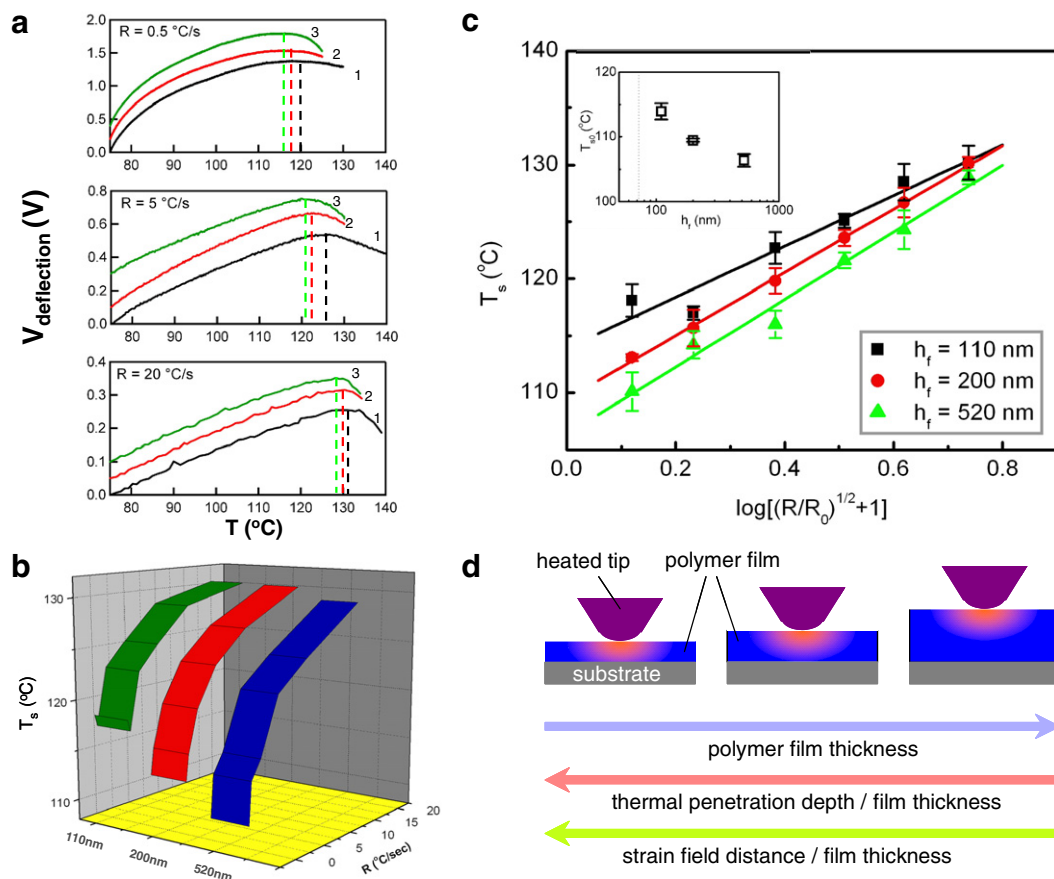


Figure 2. Non-equilibrium to quasi-equilibrium transition and size effects. (a) Nano-TM tests performed on polystyrene thin films with different thicknesses. The curves are shifted in the vertical direction. 1, 2, and 3 refer to the film thickness of 110 nm, 200 nm, and 520 nm, respectively. The three panels correspond to different ramping rates of the tip temperature. (b) 3D presentation of the influence of both film thickness and ramping rate, R , on the softening transition temperature, T_s . (c) Linear fitting of all data in (b) using the equation $T_s = T_{s0} + B \log[(R/R_0)^{1/2} + 1]$, where R_0 is 1°C s^{-1} . The error bars represent the standard deviation from 3 to 6 individual measurements of softening transition temperature. Inset shows the quasi-equilibrium 'softening temperature', T_{s0} , as a function of film thickness. The error bars represent the error from curve fitting. (d) Schematic depiction of how the thermal penetration and stress field are affected when film thickness changes.

To better understand the physical origin of the relaxation process implicit in our measurement, we extracted an apparent activation energy, E_{act} , from the Arrhenius plot of the transition temperature dependence of the ramping rate, i.e., $R = A \exp(-E_{act}/R_{gas}T_{s0})$; R_{gas} is the gas constant ($R_{gas} = 8.31 \text{ J K}^{-1} \text{ mol}^{-1}$). (Data analysis for R is provided in the supporting information (available at stacks.iop.org/Nano/19/495703) (figure S7)). As indicated in table 1, E_{act} increases monotonically from 352 to 453 kJ mol^{-1} when the film thickness decreases from 520 to 110 nm, indicating an amplified rate effect on T_s which becomes larger in thinner polymer films. The somewhat large activation energies that we observe seem to imply that segmental stress relaxation is responsible for the scanning rate dependence of the T_s shift. This is reasonable since nano-TM measurement involves plunging the nano-TM probe tip into the glassy polymer film.

It should be appreciated that nano-TM experiments involve both the thermal transfer of heat from heated tip to the film and mechanical deformation of polymer film and supported substrate. Thus, one should also account for the

Table 1. Estimation of activation energy.

Substrate	h_f (nm)	T_{s0} ($^\circ\text{C}$)	E_{act} (kJ mol^{-1})
Si	110	113.9	452.8
	200	109.5	385.8
	520	106.4	352.2
Glass	190	103.0	319.3
	500	102.2	291.3
PDMS	140	82.0	508.3
	210	83.7	427.0
	630	88.7	414.4

thermal penetration depth and the stress field induced by the contacting tip when h_f becomes smaller. Figure 2(d) schematically depicts the size effect of polymer thin films in nano-TM experiments. The heat transfer or dissipation from the tip into the polymer films determines the thermal penetration in the film. The deformation of the polymer film depends on the stress distribution. When the film thickness is decreased, the influence of both the thermal penetration

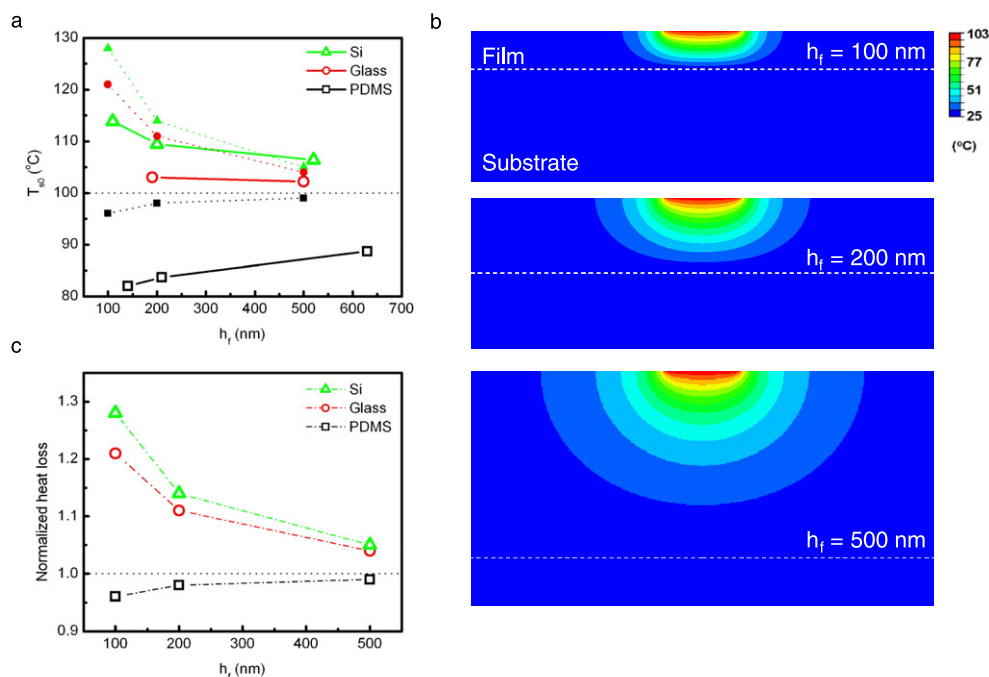


Figure 3. Substrate effect on heat dissipation. (a) Plot of T_{s0} (open symbols) and predicted tip temperature (filled symbols) versus film thickness of PS thin films on different substrates: Si, glass and PDMS. The dotted line indicates the T_g of bulk PS, i.e., $T_g = 100$ °C. (b) FEM simulation of temperature distribution in the film/substrate system at various film thickness when the heat source temperature reaches 103 °C. The film is 200 nm thick polystyrene and the substrate is silicon. The heat source is 100 nm in diameter, which is physically contacting the top surface. A sharper temperature gradient is observed for thinner film. This indicates that the heat dissipation through the substrate plays a role in nano-TM measurements. (c) Plot of the normalized heat loss versus film thickness of PS films on three different substrates.

depth and the stress field distribution relative to the film thickness should become amplified. Recognition of these basic physical effects leads us to investigate how the film thickness and substrate influence the nano-TM transition temperature through both thermal and mechanical coupling to the probe.

We investigated the change of T_{s0} for PS films supported on silicon, glass and polydimethylsiloxane (PDMS) substrates in order to study the effects of the interfacial heat transfer and the substrate mechanical stiffness. As shown in table S2 (available at stacks.iop.org/Nano/19/495703), these materials have different thermal conductivities and elastic moduli. The experimentally determined T_{s0} for different substrates (open symbols) are displayed in figure 3(a), with the horizontal dashed line indicating the T_g of the PS. In all cases the softening transition in the thicker films approaches T_g , but strong deviations are encountered in the thinner films. Notice that T_{s0} increases with thinner film on the glass and Si substrates, but *decreases* for the thinner films on the PDMS substrates. (Again, we reemphasize that all of these films are generally much thicker than those for which T_g deviations are expected.) To better understand this interesting trend we exploited finite element (FE) methods to simulate the heat transfer process. A tip–polymer contact radius of 50 nm is assumed (figure S6 in supporting materials (available at stacks.iop.org/Nano/19/495703)) while the temperature of the tip is ramped up from 75 to 103 °C in real time. Previous studies on scanning thermal microscopy concluded that the high temperatures are localized underneath the

tip [4]. The thermal contours in the cross-section of our simulations confirm that the temperature rise is strongly localized underneath the heated tip (figure 3(b)). But a steeper temperature gradient was observed for the thinner films. This implies a non-negligible role of substrate heat dissipation in the nano-TM measurement. This is further supported by plotting the total heat loss along the tip–polymer contact, into the thin film and the substrate, normalized by the total heat loss in a bulk PS surface (figure 3(c)). For the PS films on Si and glass substrates, this normalized heat loss is larger than 1, and a higher value is observed for thinner films. It is also salient that a lower heat loss is obtained for those films on glass substrates compared with comparable films on Si. This is consistent with a two order of magnitude difference between the thermal conductivity of glass and Si [5, 9]. For PS films on PDMS substrate, the normalized heat loss is slightly less than 1, and it decreases further with a decrease in the PS film thickness. This is because the thermal conductivity of the rubbery PDMS is smaller than that of the glassy polymer PS [24, 14].

The thermal conductivity of the supporting substrate is probably the most obvious factor that might influence the nano-TM softening temperature. Higher thermal conductivity substrates and thinner films allow heat to be transported away faster from the tip, raising the apparent transition temperature. If this heat transfer is the sole factor accounting for the T_s shift, the tip temperature at the contact may be estimated with the assistance of FE simulation. In the operation of a voltage-controlled heating tip, the total heat conduction through the

tip/film contact linearly scales with the total power input from the power source as all geometrical factors remain nearly unchanged. The input power is proportional to the square of the input voltage given that the electrical resistance in the heating zone remains constant. Based upon the calibration curves obtained with standard bulk materials, the tip temperature follows a quadric function of the input voltage and therefore should be proportional to the total power input as well as the heat dissipation through the contact area. FE simulations allow integration of the heat flux through the contact area and extraction of heat dissipation (loss) in the cases of different film thicknesses and substrates (figure 3(c)). Using FE modeling of the bulk material (PS films supported on a PS substrate) as a reference and assuming that the softening transition is equal to T_g , we are able to predict the tip temperature at the contact using the simulated heat dissipation. With the PS bulk T_g as 100 °C, the predicted tip temperatures are shown in figure 3(a) (the filled symbols). The predicted tip temperature does a reasonable job of capturing the experimental trends. The monotonic increase of tip temperature with decreasing film thickness on the Si and glass substrates is contrasted with the decrease of tip temperature on the soft PDMS substrates. While there are systematic differences between the measured transition temperatures and predicted tip temperatures, the general trends are correct. These differences are likely due to the heat dissipation at the tip-sample contact through the air and the meniscus layer. Nevertheless, we found that the substrate thermal dissipation is a highly relevant factor to the T_s measurement. Our comparative simulations and experiments provide a quantitative interpretation of the finite size effects on T_s measurements on PS films on silicon and glass substrates, but the large discrepancy found for soft substrates such as PDMS cannot be explained by the thermal dissipation mechanism alone. Some other factor is evidently of basic importance in our nano-TM measurements.

We next consider the effect of the mechanical properties of the supporting substrates on the T_s shift observations. Usually, the rigid substrate plays a significant role in tuning the mechanical response of the soft film once the indentation depth is over 10% of the film thickness upon indentation of a soft film on a rigid substrate. This type of substrate effect has been studied intensively for metal films [22, 25, 26, 13], and recently this phenomenon has also been reported for polymeric films, in both quasi-static and dynamic modes of testing [30, 29]. A mechanical coupling between the nano-TM probe and the substrate provides another potential contributor to T_s .

FEM simulations clearly show that there is a remarkable stress concentration in the substrate even though the stress field front has not yet approached the film-substrate interface (figure S4 in supporting materials (available at stacks.iop.org/Nano/19/495703)). At a given indentation depth, a higher effective modulus, E_{eff} , is obtained from a thinner polymer film on a rigid substrate, while a lower E_{eff} is obtained from a thinner polymer film on a soft substrate (figure 4(a)). Herein, E_{eff} was computed based on the Nix model [22] as

$$\frac{1}{E_{\text{eff}}} = \frac{1 - \nu_i^2}{E_i} + \frac{1 - \nu_f^2}{E_f} \left(1 - e^{-\frac{\alpha(h_f-d)}{a}}\right) + \frac{1 - \nu_s^2}{E_s} \left(e^{-\frac{\alpha(h_f-d)}{a}}\right), \quad (2)$$

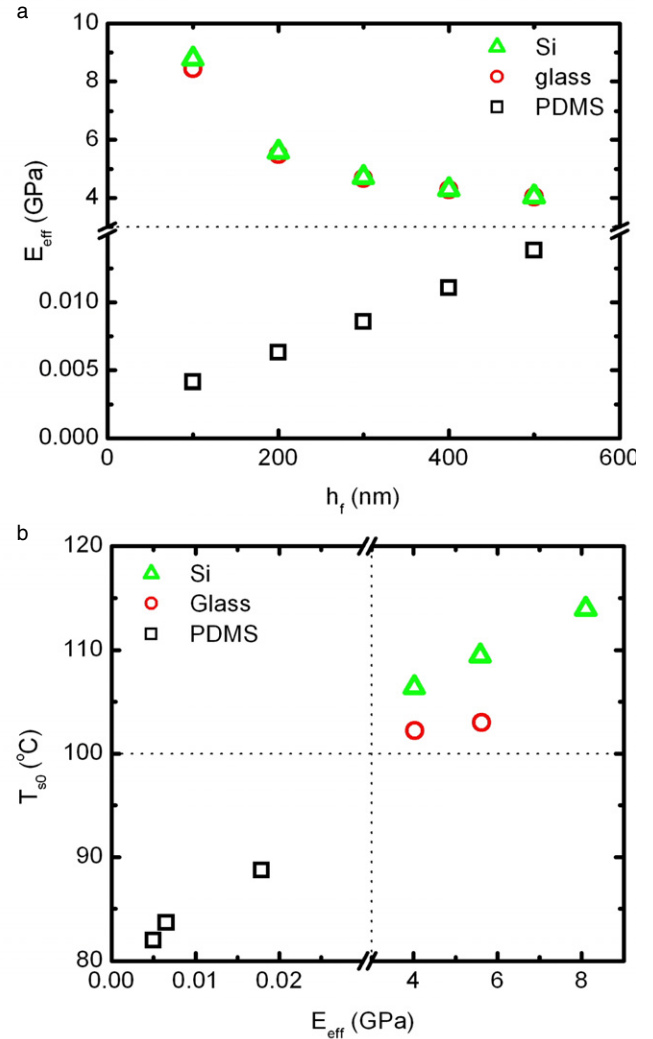


Figure 4. Intrinsic alteration of mechanical properties by the substrate effect and its influence on nano-TM transition temperature. (a) Plot of effective modulus, E_{eff} , as a function of film thickness. E_{eff} is computed based on the Nix model. The dotted lines indicate the bulk value of the elastic modulus of PS. (b) Plot of the quasi-static softening temperature, T_{s0} , as a function of E_{eff} . The dotted lines indicate the bulk value of T_g and the elastic modulus of PS.

where i, f and s refer to indenter, film and substrate properties, respectively. In this case, the indenter is silicon, so the indenter's modulus $E_i = 170$ GPa and the Poisson ratio $\nu_i = 0.25$ [22]. The film in these measurements is polystyrene ($E_{\text{PS}} = 3$ GPa and $\nu_{\text{PS}} = 0.33$) and the substrates are silicon, glass ($E_G = 73$ GPa and $\nu_G = 0.25$) [22] and PDMS ($E_{\text{PDMS}} = 2$ MPa and $\nu_{\text{PDMS}} = 0.5$) [23]. Here, d is the indentation depth, ≈ 50 nm, estimated by the pre-softening crater size and the tip geometry; a is the contact area, which is calculated from d ; h_f is the film thickness; and α is a function of $a/(h_f - d)$, using the form of a Berkovich tip [22]. This increased E_{eff} can remarkably retard the penetration of a heated tip in nano-TM experiments and consequently raise the softening transition temperature. Figure 4(b) shows how the quasi-equilibrium transition temperature, T_{s0} , changes as the E_{eff} increases owing to the confinement of the film-substrate

interface. Apparently, the greater the E_{eff} , the higher the nano-TM softening temperature becomes. Comparative study of experimental data corrected by decoupling the thermal effect will in principle provide a solution to quantitatively assess the influence of mechanical tuning and interface-induced inhomogeneity. Other mechanical coupling contributions need to be carefully examined as well. For example, the extremely low E_{eff} of PS films on PDMS substrate can result in a contact area larger than that from calibration and in turn lead to the enhanced heat loss. This also contributes to the decrease of T_{s0} , as we observed. We are currently pursuing an analytical model to decouple the thermal and mechanical properties.

4. Conclusions

We present the first systematic study of the softening of glassy polymer thin films using nano-TM with an aim of understanding puzzling observations of large softening transition temperature shifts with film thickness and variation of the film substrate. We found that thermal and mechanical coupling between the probe, the film and the substrate are responsible for the variability of the softening temperature. Environmental coupling and finite size effects can also rationalize former contradictory nano-TM softening temperature estimates. Our investigation provides the foundation for a more comprehensive physical modeling of nano-TM measurements and for more effective thermal characterization of multiphase materials and nanocomposites in practical applications. A coupling of this kind between the measurement device and the probed material is a common difficulty in nanometrology, and physically meaningful and reproducible measurements must address these coupling effects.

Acknowledgments

The authors acknowledge Dr Wen-li Wu and Dr Tianle Cheng for helpful discussions of the manuscript. Brian Berry acknowledges support from the NIST/NRC postdoctoral fellowship program. This work is an official contribution of the National Institute of Standards and Technology.

© US Government.

References

- [1] Abramson A R, Kim W C, Huxtable S T, Yan H Q, Wu Y Y, Majumdar A, Tien C L and Yang P D 2004 Fabrication and characterization of a nanowire/polymer-based nanocomposite for a prototype thermoelectric device *J. Microelectromech. Syst.* **13** 505–13
- [2] Balazs A C, Emrick T and Russell T P 2006 Nanoparticle polymer composites: where two small worlds meet *Science* **314** 1107–10
- [3] Coakley K M and McGehee M D 2004 Conjugated polymer photovoltaic cells *Chem. Mater.* **16** 4533–42
- [4] Fryer D S, Nealey P F and de Pablo J J 2000 Thermal probe measurements of the glass transition temperature for ultrathin polymer films as a function of thickness *Macromolecules* **33** 6439–47
- [5] Glassbrenner C J and Slack G A 1964 Thermal conductivity of silicon and germanium from 3 degrees K to melting point *Phys. Rev. A* **134** 1058–69
- [6] Halls J J M, Walsh C A, Greenham N C, Marseglia E A, Friend R H, Moratti S C and Holmes A B 1995 Efficient photodiodes from interpenetrating polymer networks *Nature* **376** 498–500
- [7] Hammiche A, Bozec L, Conroy M, Pollock H M, Mills G, Weaver J M R, Price D M, Reading M, Hourston D J and Song M 2000 Highly localized thermal, mechanical, and spectroscopic characterization of polymers using miniaturized thermal probes *J. Vac. Sci. Technol. B* **18** 1322–32
- [8] Huynh W U, Dittmer J J and Alivisatos A P 2002 Hybrid nanorod-polymer solar cells *Science* **295** 2425–7
- [9] Shackelford J F and Alexander W A 2001 *CRC Materials Science and Engineering Handbook* (Boca Raton, FL: CRC Press)
- [10] Keddie J L, Jones R A L and Cory R A 1994 Size-dependent depression of the glass-transition temperature in polymer films *Europhys. Lett.* **27** 59–64
- [11] King W P, Saxena S, Nelson B A, Weeks B L and Pitchimani R 2006 Nanoscale thermal analysis of an energetic material *Nano Lett.* **6** 2145–9
- [12] Lee J, Beechem T, Wright T L, Nelson B A, Graham S and King W P 2006 Electrical, thermal, and mechanical characterization of silicon microcantilever heaters *J. Microelectromech. Syst.* **15** 1644–55
- [13] Doerner M F, Gardner D S and Nix W D 1986 Plastic properties of thin films on substrates as measured by submicron indentation hardness and substrate curvature techniques *J. Mater. Res.* **1** 845
- [14] Mark J E 1999 *Polymer Data Handbook* (New York: Oxford University Press)
- [15] Moniruzzaman M and Winey K I 2006 Polymer nanocomposites containing carbon nanotubes *Macromolecules* **39** 5194–205
- [16] Nelson B A and King W P 2007 Measuring material softening with nanoscale spatial resolution using heated silicon probes *Rev. Sci. Instrum.* **78** 023702
- [17] Peumans P, Uchida S and Forrest S R 2003 Efficient bulk heterojunction photovoltaic cells using small-molecular-weight organic thin films *Nature* **425** 158–62
- [18] Pollock H M and Hammiche A 2001 Micro-thermal analysis: techniques and applications *J. Phys. D: Appl. Phys.* **34** R23–53
- [19] Reading M, Price D M, Grandy D B, Smith R M, Bozec L, Conroy M, Hammiche A and Pollock H M 2001 Micro-thermal analysis of polymers: current capabilities and future prospects *Macromol. Symp.* **167** 45–62
- [20] Rowland H D, King W P, Sun A C, Schunk P R and Cross G L W 2007 Predicting polymer flow during high-temperature atomic force microscope nanoindentation *Macromolecules* **40** 8096–103
- [21] Ruzette A V and Leibler L 2005 Block copolymers in tomorrow's plastics *Nat. Mater.* **4** 19–31
- [22] Saha R and Nix W D 2002 Effects of the substrate on the determination of thin film mechanical properties by nanoindentation *Acta Mater.* **50** 23–38
- [23] Stafford C M, Harrison C, Beers K L, Karim A, Amis E J, Vanlandingham M R, Kim H C, Volksen W, Miller R D and Simonyi E E 2004 A buckling-based metrology for measuring the elastic moduli of polymeric thin films *Nat. Mater.* **3** 545–50
- [24] Steinmetz D R 2007 Texture evolution in processing of polystyrene-clay nanocomposites *MSc thesis* Drexel University
- [25] Tsui T Y, Vlassak J and Nix W D 1999 Indentation plastic displacement field: part I. The case of soft films on hard substrates *J. Mater. Res.* **14** 2196–203

- [26] Tsui T Y, Vlassak J and Nix W D 1999 Indentation plastic displacement field: part II. The case of hard films on soft substrates *J. Mater. Res.* **14** 2204–9
- [27] Yang X and Loos J 2007 Toward high-performance polymer solar cells: the importance of morphology control *Macromolecules* **40** 1353–62
- [28] Yu G, Gao J, Hummelen J C, Wudl F and Heeger A J 1995 Polymer photovoltaic cells—enhanced efficiencies via a network of internal donor–acceptor heterojunctions *Science* **270** 1789–91
- [29] Zhou J and Komvopoulos K 2006 Surface and interface viscoelastic behaviors of thin polymer films investigated by nanoindentation *J. Appl. Phys.* **100** 114329
- [30] Zhou J and Komvopoulos K 2007 Interfacial viscoelasticity of thin polymer films studied by nanoscale dynamic mechanical analysis *Appl. Phys. Lett.* **90** 021910